Systematic Botany (2011), 36(2): pp. 470–480

DOI 10.1600/036364411X569651

Tragopogon lainzii, a New Species of *Tragopogon* (Asteraceae) Segregated from *T. dubius*: Evidence from Morphological and Molecular Data

Víctor N. Suárez-Santiago,[1,4] Consuelo Díaz de la Guardia,[1] Douglas E. Soltis,[2] Pamela S. Soltis,[3] and Gabriel Blanca[1]

[1]Departamento de Botánica, Facultad de Ciencias, Universidad de Granada, c/ Severo Ochoa, s/n, 18071 Granada, Spain.
[2]Department of Biology, University of Florida, Gainesville, Florida 32611, U. S. A.
[3]Florida Museum of Natural History, University of Florida, Gainesville, Florida 32611, U. S. A.
[4]Author for correspondence (vsuarez@ugr.es)

Communicating Editor: Andrew Hipp

Abstract—*Tragopogon dubius* is one of the most widespread species of *Tragopogon*, extending across much of Eurasia. Traditionally, *T. dubius* has been considered a morphologically homogeneous species that includes all *Tragopogon* collections with yellow flowers and swollen peduncles under capitula. Here we describe a new species of *Tragopogon* from the Iberian Peninsula, ***T. lainzii***, which has heretofore been included in *T. dubius*. To this end, we performed comparative morphological, cytogenetic, and molecular analyses on many populations of both species. Our results show that *T. dubius* is not a homogeneous species and that different lineages exist across its broad geographic distribution. Moreover, we show that hybridization has occurred in the wild between sympatric populations of *T. dubius*, ***T. lainzii***, and *T. porrifolius*.

Keywords—Cytogenetics, ETS, hybridization, ITS, morphology, *rpl16*.

Tragopogon L. includes about 150 species; the genus has a Eurasian distribution with a center of diversification in the eastern Mediterranean basin. On the Iberian Peninsula, *Tragopogon* is well represented with nine recognized species (Blanca and Díaz de la Guardia 1996; Díaz de la Guardia and Blanca 2004).

Tragopogon comprises annual, biennial, and mostly perennial herbs, with leaves entire and parallel-veined, involucral bracts in one row, and achenes muricate or scabrous and almost always with a long beak. The main morphological characters used to distinguish species involve fruit morphology, ligule color, ratio of ligule/involucral bract lengths, number of involucral bracts, and the thickness of the peduncle below the heads. *Tragopogon* is a taxonomically complex genus, and the morphological variation of the species has resulted in different interpretations by various authors; as a result, extensive taxonomic and nomenclatural confusion has occurred (reviewed in Mavrodiev et al. 2005, 2007). Hybridization is a frequent process that also increases taxonomic difficulty in the genus (Ownbey 1950; Krahulec et al. 2005); intermediate forms are commonly found in the wild where species occur sympatrically. However, hybridization is also an important mechanism of speciation in *Tragopogon*, especially when associated with polyploidy (Ownbey 1950; Ownbey and McCollum 1953; Díaz de la Guardia and Blanca 1990; 2004; Soltis et al. 2004; Mavrodiev et al. 2008a, b).

Tragopogon dubius Scop. (section *Majores* Kuth.) is one of the most widespread species of *Tragopogon*, extending across much of Eurasia. The species is mainly characterized by its pale yellow ligules, all shorter than the involucral bracts, with commonly eight to 12 involucral bracts, and strongly inflated peduncles below the heads. However, the recognition of this species is usually restricted to those plants that are yellow-flowered and have swollen peduncles. In this delineation, other important characters (e.g. achene morphology and ratio of ligule/involucral bract lengths) are underutilized. As a result, the true extent of intraspecific morphological variability has been underestimated, which may even mask the presence of other yellow-flowered and swollen-peduncled species under the name *T. dubius*. In fact, unlike *T. porrifolius* L. (another widespread *Tragopogon* species; see Mavrodiev et al. 2007), *T. dubius* has often been considered a morphologically homogeneous species, and few nomenclatural problems have involved this species. Jacquin (1773), using material from Austria, proposed *T. major* Jacq. to include those plants like *T. dubius* but with wide leaves, large heads, and 10–12(–18) involucral bracts; Chaubard (1837) and Lindemann (1881) described new varieties for *T. major* (var. *decipiens* Chaub. ex Noulet; var. *desertorum* Lindem.). However, most authors later considered *T. major* a synonym of *T. dubius*, because the diagnostic characters for *T. major* are not sufficiently distinct to warrant its recognition. Thus, Vollmann (1914) considered *T. major* as a subspecies of *T. dubius* [subsp. *major* (Jacq.) Vollmann], while Bolòs and Vigo (1989) treated it as a variety of *T. dubius* [var. *major* (Jacq.) Bolòs & Vigo; var. *decipiens* (Chaub. ex Noulet) Bolòs & Vigo]. Tzvelev (1985) combined the variety described by Lindemann for *T. major* as a subspecies of *T. dubius* [subsp. *desertorum* (Lindem.) Tzvelev]. Richardson (1976), in his review for *Flora Europaea*, did not recognize any infraspecific taxonomic units within *T. dubius* and considered *T. major* a synonym of *T. dubius*.

Recent evidence from molecular analyses seems to refute the supposed homogeneity for *T. dubius* across its geographic distribution. For example, what has been called *T. dubius* from India seems to be genetically, as well as morphologically, distinct from the European *T. dubius* and appears to warrant recognition as a new species (Mavrodiev et al. 2008a).

Thus, specimens referred to as *T. dubius* from different geographic areas may represent distinct, previously unrecognized species. Observations of collections in nature first suggested to us that plants recognized as *T. dubius* from southern Spain likely represented a separate entity, morphologically distinct from other collections of *T. dubius*. In this study, we describe a new species of *Tragopogon* from the Iberian Peninsula, *T. lainzii*, which has traditionally been considered as *T. dubius*. To this end, we performed comparative morphological, cytogenetic, and molecular analyses on multiple populations of both species. Moreover, we show that hybridization has occurred in the Iberian Peninsula between sympatric species of *Tragopogon*, involving both *T. dubius* and *T. lainzii*, as well as more distantly related species such as *T. porrifolius*.

Materials and Methods

Morphology—A comparative analysis of morphological characteristics was performed on 17 populations (eight of "typical" *T. dubius* and nine of the putative new species) across their distribution in the Iberian Peninsula (Appendix 1, Fig. 1). Two of the 17 populations analyzed were not included in the statistical analyses because they were determined to be hybrid populations (see Results) and the morphology of these individuals was influenced by the species involved in the hybridizations. Characters used in the morphological analysis (quantitative and qualitative) were those exhibiting the greatest variation between the two putative species (18 quantitative and five qualitative characters; Table 1). Flower characters were measured during anthesis of middle-inflorescence flowers, while achene characters were measured on mature achenes from the peripheral flowers of the capitulum. The achenes were photographed using a variable-pressure LEO 1430 VP scanning electronic microscope (SEM) in conventional mode, after gold–palladium coating (Thornill et al. 1965). The terminology used basically follows Font Quer (1979) and Stearn (1980).

The statistical program used for analyses was SPSS version 15.0.1 (SPSS, Inc., Chicago, Illinois). Because our data are not normally distributed, we applied a Mann-Whitney *U* test for each of the quantitative variables studied to test for differences between *T. dubius* and the putative unrecognized species. To check for intraspecific and interpopulation homogeneity of the quantitative morphological characters a data matrix was produced from the 18 characters studied and subjected to a clustering analysis (the qualitative characters were constant within each putative species and hence not included in this analysis). To construct the data matrix, the population average value for each continuous quantitative character was calculated. A logarithmic transformation of these average values was performed [log $(x + 1)$]. The clustering method used was UPGMA (Unweighted Pair-Groups Method using Arithmetic averages), using a dissimilarity matrix generated with Euclidean distances. We used this hierarchical clustering method because it permitted us to check for structure in the morphological diversity between populations.

Karyological Analysis—Chromosome numbers were counted at metaphase in root-tip meristems taken from germinating seeds. Roots were pretreated with 8-hydroxy-quinoline, fixed in ethyl alcohol–acetic acid (3:1), hydrolysed in 1 N HCl, stained in acetic orcein solution, and then flattened for light microscopy (Darlington and La Cour 1969).

Chromosomes were matched and paired based on centromere position and size, and the karyotypes were represented by their chromosomal formula. For chromosome nomenclature we followed that proposed by Levan et al. (1964), and for quantification of karyotype symmetry we followed the classification of Stebbins (1971).

Molecular Analysis—The internal transcribed spacer region (ITS-1, 5.8S, ITS-2; hereafter ITS) and the 3′portion of the external transcribed spacer (Lee et al. 2002; hereafter ETS) of the nuclear ribosomal (nr) DNA, as well as the first intron of the *rpl16* chloroplast gene, were used as molecular markers. Intraspecific variability of *T. dubius* and the putative segregate was explored by sequencing individuals from different populations. In addition to the populations studied from a morphological standpoint, in the molecular analysis we included other populations of *T. dubius* and the putative unrecognized species (Appendix 1). To facilitate placement of the latter samples with their closest relatives, we included sequences of representative species of the Majores s. l. clade (following the phylogeny of *Tragopogon* by Mavrodiev et al. 2005). These sequences were either taken from GenBank or generated as part of this study from Iberian taxa. *Tragopogon olympicus* Boiss. was selected as an outgroup based on its position as sister to the remainder of the Majores clade in the aforementioned phylogeny. EMBL accession numbers for the new sequences are given in Appendix 1, while the GenBank accession numbers for the remainder are given on the phylogenetic trees.

Total genomic DNA was extracted, using the CTAB method (Doyle and Doyle 1987), from fresh leaves collected in the wild. The entire ITS region (ITS-1, 5.8S and ITS-2), the 3′portion of the ETS and the plastid

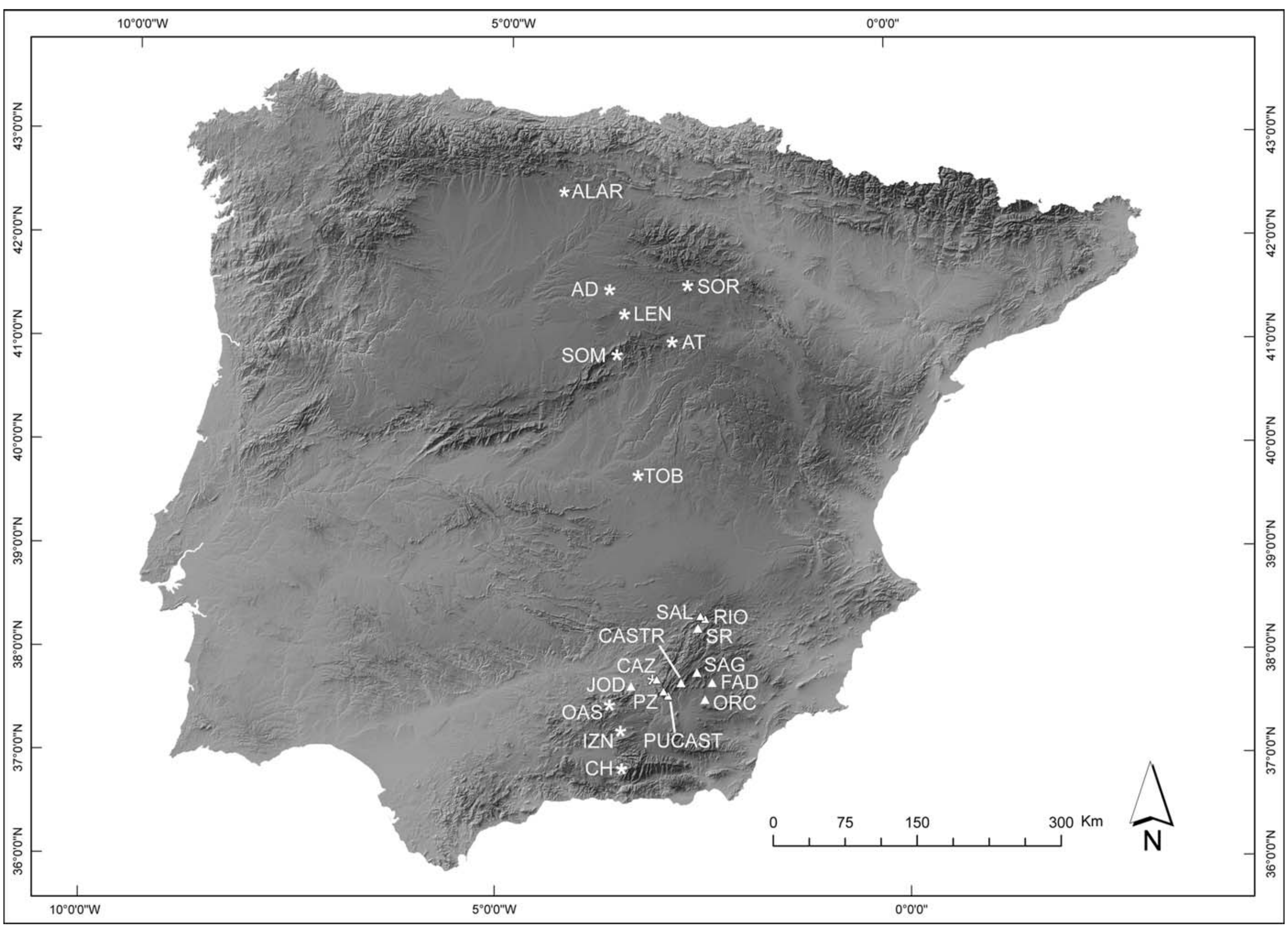

Fig. 1. Map of the Iberian Peninsula showing the localities sampled of *T. dubius* (asterisk) and *T. lainzii* (triangle). See Appendix 1 for population codes.

TABLE 1. Principal morphological characters distinguishing *T. dubius* and *T. lainzii*. Results of biometric analysis are shown: interval of extreme values, mean (± 1 s. e.), N = number of samples analysed and *p* values obtained by Mann-Whitney *U* test (significant *p* values are marked with an asterisk).

Character	*T. dubius*	*T. lainzii*	*p* value
Stem color	Greenish	Reddish	
Leaf margin	Not-undulate	Undulate	
Peduncle width at anthesis (mm)	6–12 [8.80 ± 0.13 (N = 95)]	7–13 [10.05 ± 0.13 (N = 110)]	0.000*
Peduncle width in fruit (mm)	12–20 [14.85 ± 0.14 (N = 97)]	12–20 [14.88 ± 0.15 (N = 102)]	0.932
Bud shape	Triangular	Ovate-oblong	
No. of involucral bracts	7–14 [9.64 ± 0.15 (N = 155)]	9–16 [13.00 ± 0.02 (N = 245)]	0.000*
Involucral bract length at anthesis (mm)	29–45 [37.99 ± 0.24 (N = 210)]	27–45 [34.32 ± 0.21 (N = 282)]	0.000*
Involucral bract length in fruit (mm)	55–85 [63.40 ± 0.37 (N = 180)]	44–66 [54.79 ± 0.29 (N = 252)]	0.000*
Involucral bract width at anthesis (mm)	4–7 [5.53 ± 0.04 (N = 210)]	4–9 [5.7 ± 0.06 (N = 282)]	0.239
Involucral bract width in fruit (mm)	7–11 [8.65 ± 0.06 (N = 180)]	5–11 [7.92 ± 0.05 (N = 252)]	0.000*
Ligule length (mm)	16–33 [23.25 ± 0.27 (N = 210)]	30–48 [37.29 ± 0.20 (N = 282)]	0.000*
Ligule length/ involucral bract length	0.45–0.82 [0.61 ± 0.01 (N = 210)]	0.93–1.43 [1.09 ± 0.00 (N = 282)]	0.000*
No. of achenes per head	49–134 [91.75 ± 0.02 (N = 28)]	115–263 [186.30 ± 0.02 (N = 23)]	0.000*
Total achene length (mm)	23.5–33.5 [29.52 ± 0.13 (N = 210)]	25–38.5 [31.50 ± 0.19 (N = 252)]	0.000*
Achene-body length (mm)	11–14 [12.12 ± 0.04 (N = 210)]	7.5–11.5 [9.96 ± 0.05 (N = 252)]	0.000*
Achene-body width (mm)	1.5–2.3 [1.90 ± 0.01 (N = 210)]	1–1.7 [1.31 ± 0.01 (N = 252)]	0.000*
Achene-body length/achene-body width	5–8.13 [6.41 ± 0.04 (N = 210)]	6–11 [7.66 ± 0.05 (N = 252)]	0.000*
Achene-beak length (mm)	10.5–21.5 [17.40 ± 0.13 (N = 210)]	15.5–27.5 [21.53 ± 0.17 (N = 252)]	0.000*
Achene-beak length/achene-body length	0.78–1.87 [1.44 ± 0.01 (N = 210)]	1.45–2.89 [2.17 ± 0.02 (N = 252)]	0.000*
Achene ornamentation	Coarse-ornamented	Fine-ornamented	
Apex-beak shape	Bulbous	Obpyramidal	
Pappus length (mm)	18–27 [22.86 ± 0.14 (N = 210)]	20–30 [23.98 ± 0.12 (N = 252)]	0.000*
Achene length/pappus length	1–1.67 [1.30 ± 0.01 (N = 210)]	1.06–1.65 [1.31 ± 0.01 (N = 252)]	0.090

rpl16 intron were amplified by PCR, using primers N-nc18S10 and C26A (Wen and Zimmer 1996) for the ITS region, L-ETS (Lee et al. 2002) and 18S-ETS (Baldwin and Markos 1998) for ETS, and rpL16F71 (Jordan et al. 1996) and rpL16R1516 (Small et al. 1998) for the *rpl16* intron. Amplification reactions were performed in a volume of 50 µl, under standard conditions (Innis et al. 1990) for ITS and ETS, and following Small et al. (1998) for the *rpl16* intron. Automated sequencing of the purified PCR products was performed in both directions using the amplification primers on a 3100-Avant Genetic Analyzer (Applied Biosystems, Inc., Foster City, California).

Nucleotide sequences were edited and aligned with the SEQMAN II v. 3.61 and MEGALIN v. 3.18 programs, respectively, from the DNAstar software package (DNASTAR, Inc., Madison, Wisconsin) and then adjusted by eye. To estimate the extent of sequence identity (intra and interspecific), we calculated the divergence (uncorrected *p*-distance) between sequences using MEGA v. 4 (Tamura et al. 2007).

Phylogenetic analyses were performed using two optimality criteria: maximum parsimony (MP) as implemented in PAUP* v. 4.0b10 (Swofford 2003) and Bayesian inference using MrBayes v. 3.1.2 (Ronquist and Huelsenbeck 2003). Separate analyses were conducted on the ITS, ETS and *rpl16* data sets, with an additional analysis on the combined ITS + ETS matrix. The data matrices are available from TreeBASE (study number S10410).

Parsimony analyses involved heuristic searches. The data matrices were subjected to 1,000 replicates of random sequence additions using tree bisection-reconnection (TBR) branch-swapping under the Fitch criterion (unordered states and equal weights). Gaps were treated as missing data. Potentially phylogenetically informative and unambiguously aligned gaps (there were no ambiguous regions in the alignment) were coded as individual characters and subjected to specific step matrices following the method proposed by Lutzoni et al. (2000) and using the program INAASE v. 3 (Lutzoni et al. 2000). Only ten trees were held at each step, to minimize the time spent searching for trees on suboptimal islands. The starting tree was obtained by stepwise addition. Finally, 1,000 bootstrap replicates (BS: Felsenstein 1985) with 10 heuristic searches, as above, were performed to assess internal support for nodes. Statistics reflecting the amount of phylogenetic signal in the parsimony analysis were provided by the consistency index (CI: Kluge and Farris 1969) and the retention index (RI: Swofford 1993).

Bayesian analyses were implemented using the best-fit nucleotide substitution model for each data set [HKY (nst = 2; rates = equal; statefreqpr = dirichlet) for ETS, K80 + G (nst = 2; rates = gamma; statefreqpr = fixed) for ITS, and F81 + I (nst = 1; rates = propinv; statefreqpr = dirichlet) for *rpl16*]. These models were selected using MrModeltest 2.3 (Nylander 2004) and the Akaike information criterion (Akaike 1973). For the ETS + ITS combined analysis a partitioned model was used, which included the selected models for the independent data sets. The analyses were based on 5,000,000 generations with four simultaneous runs (sixteen Markov chain Monte Carlo, MCMC, chains) starting from random trees that were sampled every 100 generations. To determine apparent stationarity of the runs the variation in log-likelihood scores was examined graphically. The initial 25% of the samples obtained were discarded as burn-in. Convergence was assessed checking the standard deviation of split frequencies for the four independent runs and also graphically using the slide command (it shows the posterior probabilities of clades for nonoverlapping samples of trees in the sample) and compare command (it plots pairwise split frequencies for a series of independent MCMC runs) of the program AWTY online (Wilgenbusch et al. 2004). As for the parsimony analyses, those potentially informative gaps were treated as individual characters, and the standard discrete model was specified for them.

Results

Morphology—The results of the biometric analysis, as well as the main qualitative morphological characters, differentiate between *T. dubius* and the putative new species (Table 1, Fig. 2). Because the data support the segregation of a new species from *T. dubius*, we will henceforth refer to it as *T. lainzii*; a formal description appears in the Taxonomic Treatment. The main differences between the species involve both floral and achene characters, as well as leaf features. *Tragopogon lainzii* always possesses longer ligules than does *T. dubius*, with the ligules as long as or longer than the involucral bracts in *T. lainzii* (Fig. 3), while in *T. dubius* the involucral bracts always exceed the ligules. The number of involucral bracts is almost constant (13) in *T. lainzii*, while in *T. dubius* the number frequently varies from (7–)8–12(–14). Although the achene length is similar in both species, *T. lainzii* differs from *T. dubius* in having an achene-beak that is longer and an achene-body that is shorter and thinner. Moreover, *T. lainzii* characteristically possesses a fine-ornamented achene with an obpyramid-shaped apex-beak, while *T. dubius* has a coarse-ornamented achene with a bulbous-shaped apex-beak (Fig. 4). Furthermore, *T. lainzii* always has undulate leaves, while the leaves are not undulate in *T. dubius* (Fig. 3), and the number of

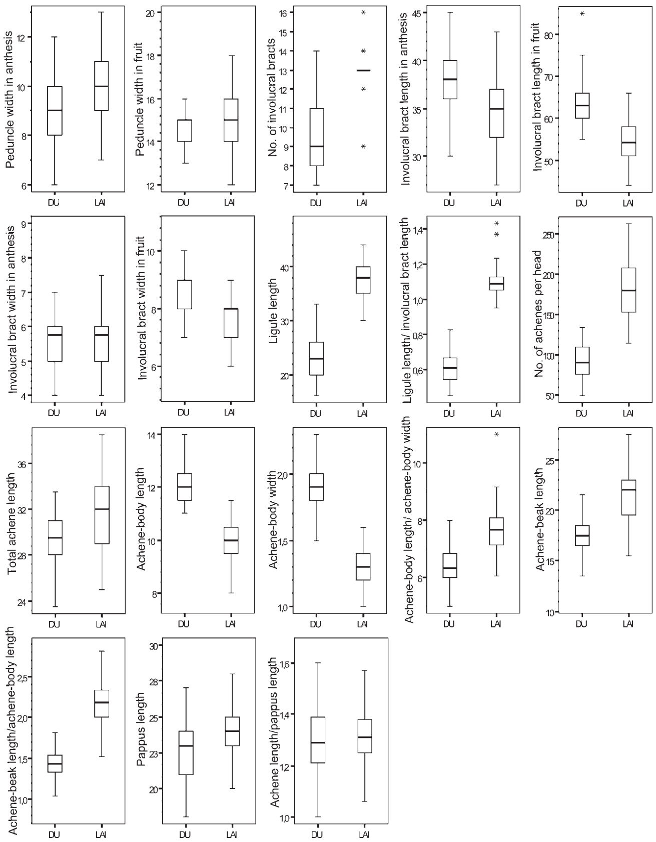

Fig. 2. Box plots of the distributions of the 18 morphological quantitative characters for *T. dubius* (DU) compared with *T. lainzii* (LAI). Measurements are expressed in mm. *: extreme values.

achenes per head is higher in *T. lainzii* than in *T. dubius* (Table 1). Statistically significant differences were found ($p < 0.001$) in almost all quantitative characters, except for involucral-bract width during flowering, ratio between the lengths of the achene and pappus, and the peduncle width during ripening (Table 1). UPGMA analysis likewise supports the morphological separation of *T. lainzii* and *T. dubius* (Fig. 5).

Karyological Analysis—All populations of *T. lainzii* studied exhibited the diploid chromosome number for the genus ($2n = 12$). Figure 6 shows both a metaphase plate as well as the karyotypes for *T. lainzii* and *T. dubius*. Both species possess a similar bimodal karyotype, having three chromosome pairs each with a submedian centromere and three chromosomal pairs each with a median centromere.

A secondary constriction is always found in the first chromosome pair, constituting a satellite in its short arm. Chromosomal formula: $2n = 12 = 2\text{sm sat} + 4\text{sm} + 6\text{m}$. Karyotype asymmetry is of the 2B type (2: 51–99% of chromosomes with an arm ratio < 2:1; B: ratio between the largest and the smallest chromosome of 2:1–4:1). Neither species exhibited any intraspecific chromosomal variation. There are no obvious karyotypic differences between the two species.

Molecular Analysis—Alignment of all 46 ETS sequences resulted in a 535-bp data matrix. The ITS-5.8S matrix is 728 bp in length and consists of 49 sequences, and the *rpl16* matrix is 1,087 bp in length and includes 33 sequences. The ETS + ITS combined matrix includes all ETS and ITS sequences (51) and is 1,263 bp in length; in this matrix six accessions were only represented by one of the two regions (only by ETS: collections of *T. porrifolius* from population CAZ ; only by ITS: *T. dubius* from Germany, AJ633503, and from Switzerland, AJ633500, *T. porrifolius* from Germany, AJ633494, and from Italy, EF374206, and *T. kraschenninikovii*, AY645821). To check the possible impact of including these six accessions on the resulting topology, the analysis was repeated including only those taxa for which both regions were available. The resulting topology was concordant with that obtained including taxa with only one type of sequence and the support of the clades did not vary substantially (data not shown).

Parsimony analysis of the ITS sequences yielded 5,730 most-parsimonious trees (length: 102, CI: 0.912, RI: 0.940), while 54,216 trees were obtained for the ETS matrix (length: 71, CI: 0.958, RI: 0.990), and 23,967 trees were obtained for the combined ETS + ITS matrix (length: 180, CI: 0.894, RI: 0.960). Parsimony analysis of the *rpl16* data set reached the maximum number of trees permitted in memory (length: 69, CI: 0.928, RI: 0.951). The resulting strict consensus topologies were all similar to those obtained via Bayesian inference. The analyses of the nrDNA regions (ETS, ITS) resulted in no contradictory topologies, because the main differences between them were due to the higher resolution shown by the ETS sequences to resolve the phylogeny at internal nodes (data not shown). The combined analysis of these two regions yielded an almost completely resolved phylogeny (Fig. 7).

The ETS + ITS tree shows three highly supported clades that correspond to the three main subclades (Majores s. s., Chromopappus, and Hebecarpus) within the Majores s. l. clade. Sequences of the different populations of *T. lainzii* are identical for both ETS and ITS and form a strongly supported clade (BS: 98%, PP: 1.00); these populations are included in the core of the Majores s. s. clade and are clearly separated from the clade formed by the Spanish populations of *T. dubius*. Sequences from one population of *T. lainzii* (RIO) are included in the *T. dubius* clade (Fig. 7), showing a high identity with the sequences of the latter (ETS: 100%, ITS: 99.9–100%). Two additional sequences were also placed in clades that contradicted their morphology (Fig. 7): one of them was amplified from an individual of *T. porrifolius* (population CAZ), but was placed in the Spanish *T. dubius* clade (99% identity); the other was obtained from a *T. dubius* individual (population CH) and is related to *T. porrifolius* in the Hebecarpus clade (100% identity).

The phylogenetic tree places populations of *T. dubius* in different clades (Fig. 7). Sequences of *T. dubius* from Turkey (including *T. major*) and from Switzerland are included in the core of the Majores s. s. clade, while *T. dubius* from Spain appears as a sister group to the latter. Finally, *T. dubius* from India and one collection from Germany form a group not related to the Majores s. l. clade.

The *rpl16* intron yielded trees (Fig. 8) less resolved than those obtained with the nrDNA markers. Like the ETS + ITS tree, the *rpl16* tree shows a strongly supported *T. lainzii* clade. However, unlike the nrDNA tree, the chloroplast tree shows a close relationship between *T. lainzii* and *T. dubius* from Spain [even more closely related than the sequence of *T. dubius* from Turkey, EU392002 (from the same individual as ETS sequence AY645859 and ITS sequence AY645813; see Fig. 7)]. The sequence of *T. lainzii* from population RIO and the *T. dubius* sequence from population CH show the same relationships as those shown in the ETS + ITS tree (Figs. 7, 8); however, the sample of *T. porrifolius* from the CAZ population is related to the other *T. porrifolius* sequences (Fig. 8) instead of to the *T. dubius* ones (unlike in the ETS + ITS tree; Fig. 7).

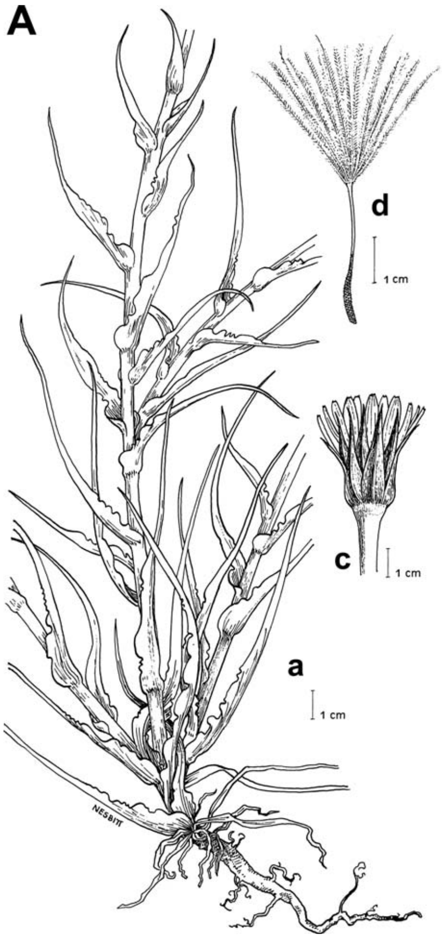

Fig. 3A. *Tragopogon lainzii* (GDA 52778, holotype), a: general appearance, b: flowering head, c: ripening head, d: achene.

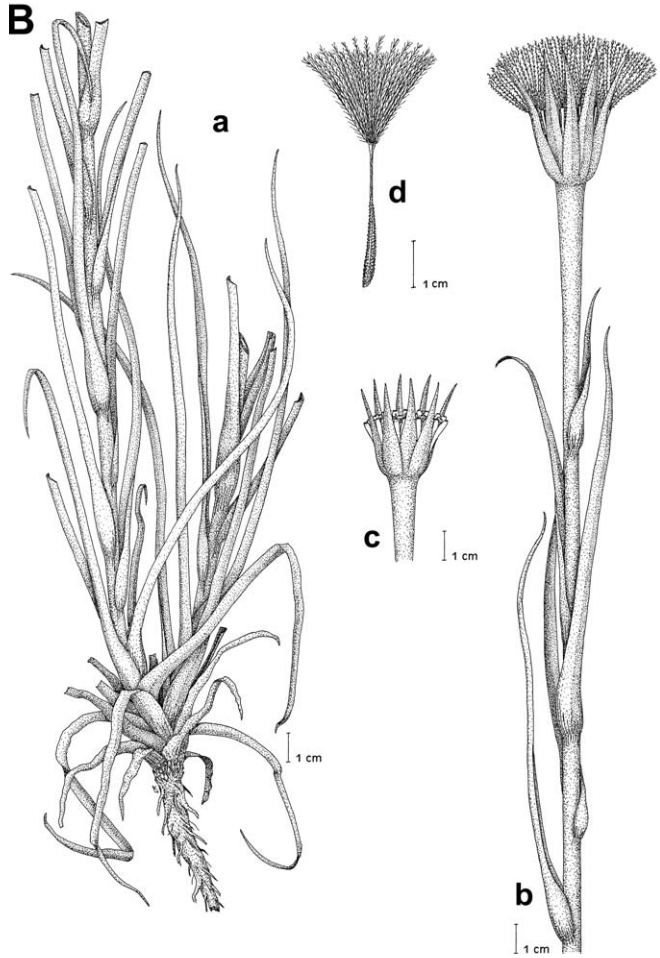

Fig. 3B. *Tragopogon dubius* (GDA 54996), a: general appearance, b: flowering head, c: ripening head, d: achene.

Divergent Populations—In the morphological analysis we detected one population of *T. lainzii* and one of *T. dubius* in which the individuals showed anomalous character states with regard to the other populations. These populations are the same ones that did not group by taxonomy in the molecular trees (RIO of *T. lainzii*, and CH of *T. dubius*; Figs. 7, 8). Individuals from RIO always showed the floral morphology typical of *T. lainzii*. Moreover, the individuals from this population always showed undulate leaves like *T. lainzii*. However, the features of the achenes were variable within this population; we could find achenes typical of *T. lainzii*, but also achenes typical of *T. dubius* (coarse-ornamented with an achene-beak shorter and an achene-body longer and thicker, respectively, than typical of *T. lainzii*). Also an intermediate gradation between species was found for achene characters.

Despite the presence of yellow flowers in the individuals from the CH population, these plants showed different values for almost all other morphological characters compared to those typical (Table 1) of the individuals from other populations of *T. dubius* (e.g. mean values: ligule length at anthesis: 29.23 mm, ratio ligule length/bract length: 0.757, total achene length: 33.35 mm, achene-beak length: 21.7 mm, ratio beak length/body length: 1.87). The qualitative characters of individuals from the CH population (e.g. undulate leaves, the fine-ornamented achenes, and a (sub)cylindrical apex-beak shape) were also different compared to other populations of *T. dubius*.

Finally, after obtaining the molecular results, we checked the morphology for individuals of *T. porrifolius* from population CAZ (another population that did not group by taxonomy in the molecular trees; Fig. 7). In this case we found variability in achene morphology; in the extreme cases the achenes were similar to those of *T. dubius*.

All sampled individuals from these three populations were diploids and showed the same karyotype found in *T. dubius* and *T. lainzii*.

Discussion

Taxonomic Characterization of T. lainzii—*Tragopogon lainzii* is a newly described diploid species of *Tragopogon* (see Taxonomic Treatment) that can be distinguished morphologically from *T. dubius* by the following: the tinge color on the stems, margin of the leaves, shape of the capitula, number of involucral bracts, length of the ligules as a proportion of the length of the involucral bracts, ornamentation of the achene surface and the shape of the apex of the beak (Table 1; Figs. 2, 3). With regard to the number of involucral bracts, except for two cases, *T. lainzii* always showed a constant number of 13, while in *T. dubius* this number was more variable, ranging from (7–)8–12(–14) with eight the most common number. Among the aforementioned characters some of the most important morphological characters to distinguish the species

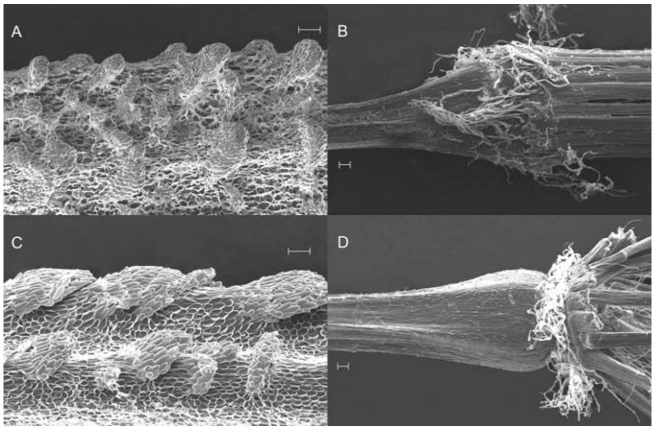

FIG. 4. Scanning electron micrographs (SEM) of achenes of *T. lainzii*, GDA 52778, holotype (A, body of achene; B, apex of beak) and *T. dubius*, GDA 54996 (C, body of achene; D, apex of beak). Scale bar = 100 µm.

of *Tragopogon* are the length of the ligules relative to the length of the involucral bracts, the number of involucral bracts and the characters derived from the achenes (Blanca and Díaz de la Guardia 1997). Moreover, there are other important characters that, in spite of some overlap in their measurements, nonetheless distinguish *T. lainzii* from *T. dubius*. Thus, *T. lainzii* in general shows shorter involucral bracts during achene ripening, a shorter and more slender achene body and more achenes per head than does *T. dubius* (Table 1).

Both the quantitative analysis and UPGMA phenogram support the taxonomic recognition and characterization of *T. lainzii* (Table 1; Fig. 5). The phenogram shows that the populations of each species group together by morphological similarity, indicating the interpopulational homogeneity of the morphological characters of this new species.

Karyologically, no differences were found between the populations of *T. lainzii* and *T. dubius*; all studied individuals showed the same chromosomal formula: $2n = 12 = 2sm\ sat + 4sm + 6m$ (Fig. 6).

Other Iberian species of *Tragopogon* with yellow flowers are *T. lamottei* Rouy, *T. pratensis* L., and *T. pseudocastellanus* Blanca & C. Díaz. However, *T. lainzii* can be easily distinguished from them based on morphological (see key to yellow-flowered species in the Iberian Peninsula) and, in the case of *T. pseudocastellanus*, which is polyploid with $2n = 24$, cytological features (Blanca and Díaz de la Guardia 1996).

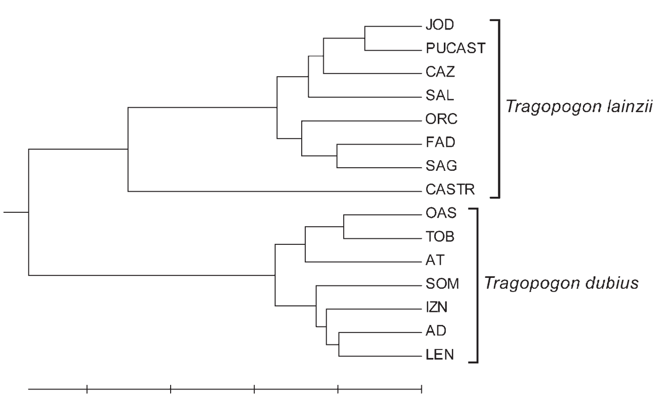

FIG. 5. UPGMA phenogram obtained from the Euclidean distances calculated for 18 morphological quantitative characters in 15 populations of *T. lainzii* and *T. dubius* of the Iberian Peninsula.

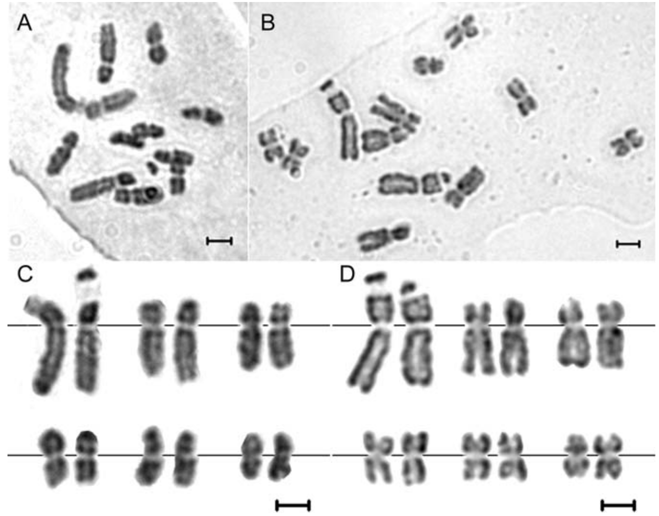

FIG. 6. Metaphase plates and karyotypes of *T. lainzii* (A, C) and *T. dubius* (B, D). Scale bar = 2 µm.

Phylogenetic Analysis—All phylogenetic analyses support the recognition of *T. lainzii* as an independent species from the morphologically similar species, *T. dubius*. Importantly, all sequences of *T. lainzii* (exceptions discussed below) formed a strongly supported clade separated from *T. dubius*, for all molecular markers used.

Contrary to the meaning of the specific epithet (dubius = doubtful), *T. dubius* has long been considered morphologically homogeneous by taxonomists, with invariant morphological characters. Thus, the traditional concept of *T. dubius* has included all *Tragopogon* species with yellow flowers and swollen peduncles under the capitula (e.g. Vollmann 1914; Richardson 1976; Tzvelev 1985; Bolòs and Vigo 1989). Our results show that *T. dubius* is not morphologically homogeneous and the specific epithet is well deserved. *Tragopogon lainzii* has been considered part of *T. dubius*, and it illustrates that not all yellow-flowered *Tragopogon* with swollen peduncles are *T. dubius*. In fact, distinct lineages, to date unrecognized as species, may be included under this broad concept of *T. dubius*. Mavrodiev et al. (2008a), studying the parentage of the tetraploid *T. kashmirianus* G. Singh, suggested that *T. dubius* from India and neighboring countries may be a different species from the European *T. dubius*, on the bases of molecular and morphological data. Our phylogenetic analyses agree with Mavrodiev et al. (2008a) and show *T. dubius* as a nonmonophyletic species, with different lineages existing across its geographic distribution. Thus, in addition to the distinctiveness of *T. lainzii*, other samples of *T. dubius* from the Iberian Peninsula are not part of the same subclade as other sampled European (Switzerland, AJ633500) and Turkish (including *T. major*) *T. dubius*. While the latter are included in the core of the Majores s. s. clade (sensu Mavrodiev et al. 2005), the sequences of the Iberian populations form a sister clade to the Majores s. s. clade. Finally, the sequence of the *T. dubius* collection from India used by Mavrodiev et al. (2008a) appeared closely related to a sequence from Germany and clearly is not related to the species of the Majores s. l. clade [in Mavrodiev et al. (2008a), *T. dubius* from India occurred in a clade of native species from Kashmir, which is sister to the *Tragopogon* clade sensu Mavrodiev et al. (2005)]. This relationship between *T. dubius* from India and one collection from Germany would increase the range of the putative new Indian

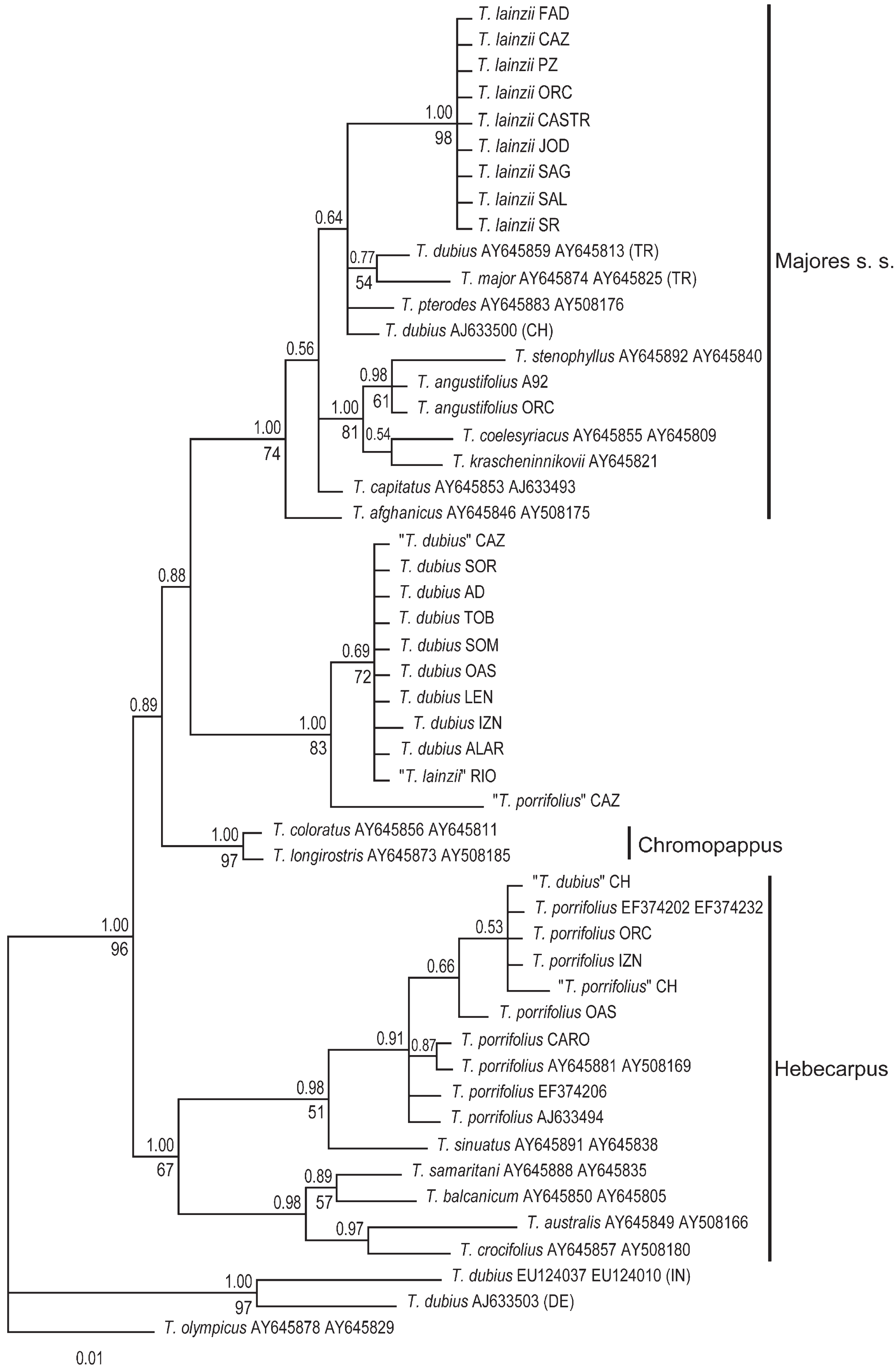

Fig. 7. Bayesian consensus tree for analysis of the ETS + ITS data set for studied species of *Tragopogon*. Numbers above branches are posterior probabilities, and numbers below branches are bootstrap values ≥ 50% obtained in the parsimony analysis, which generated the identical topology. Specific epithets for sequences from hybrid populations are in quotes. Country codes (in parentheses) for non-Spanish *T. dubius* populations: CH: Switzerland; DE: Germany; IN: India; TR: Turkey; see Appendix 1 for Spanish population codes of the sequences generated in this study. Names for clades within Majores s. l. are taken from Mavrodiev et al. (2005).

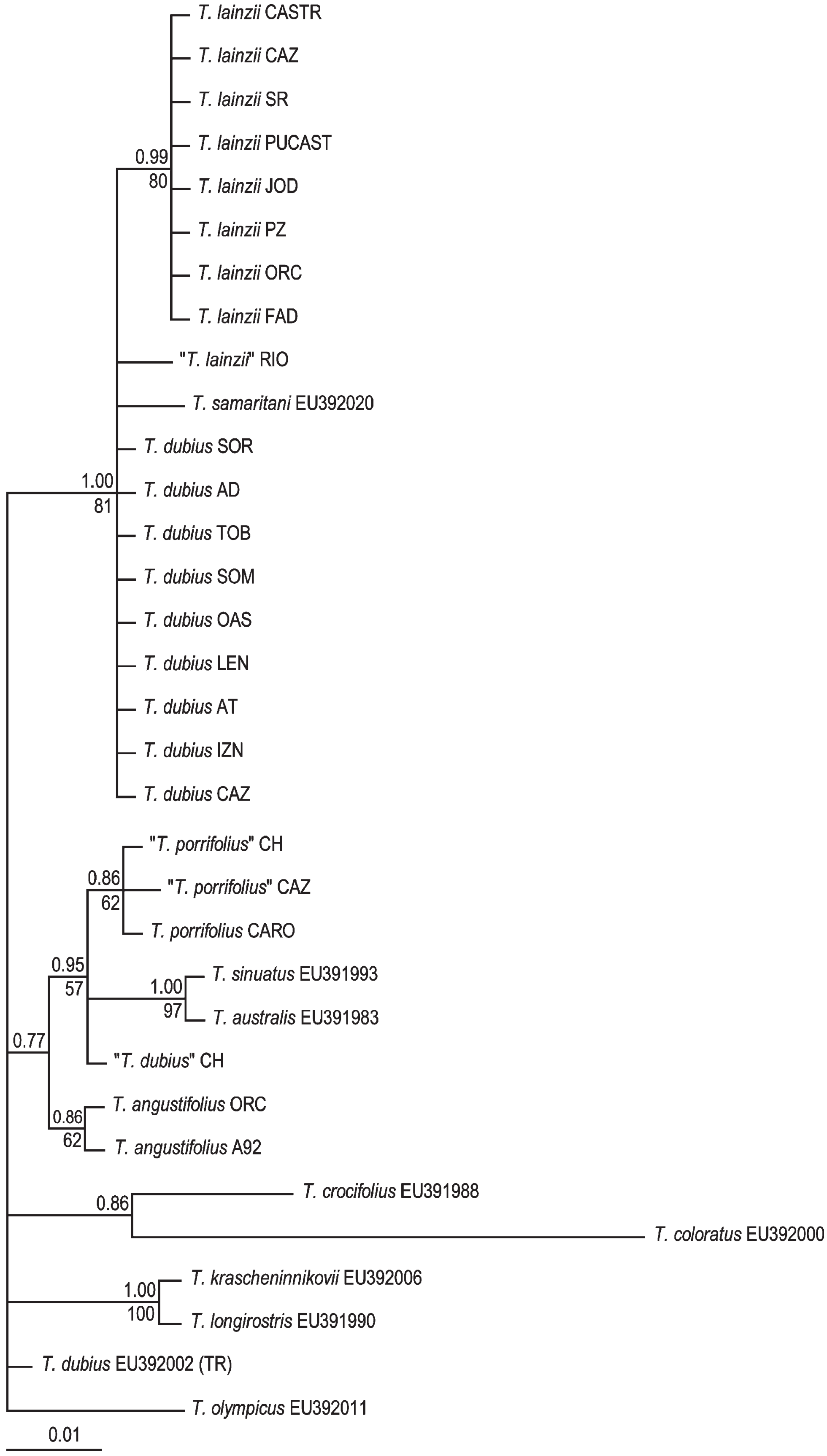

FIG. 8. Bayesian consensus tree for analysis of the plastid *rpl16* sequences of the studied *Tragopogon* species, showing the same topology as the 50% majority tree obtained in the parsimony analysis. Numbers above branches are posterior probabilities, and numbers below branches are bootstrap values ≥ 50%. Specific epithets for sequences from hybrid populations are in quotes. Country codes (in parentheses) for non-Spanish *T. dubius* populations: TR: Turkey; see Appendix 1 for Spanish population codes of the sequences generated in this study.

species (suggested by Mavrodiev et al. 2008a). Clearly more sampling and study of this material is needed.

Karyological studies of *T. dubius* by Dvořák et al. (1978) showed two different karyotypes in different populations. Thus, one of these two karyotypes was the same as that reported here in the Iberian populations of *T. dubius* (6sm + 6m), while the other ones differed in having 8, instead of 6, chromosomes with the centromere in median position (4sm + 8m). Thus, other unrecognized cryptic species may exist within what is now called *T. dubius*.

The molecular differentiation of plants of *T. dubius* from Spain compared to the taxa of the Majores s. s. clade, as well as the nonmonophyletic nature of *T. dubius* throughout its geographic distribution and the reported variation in karyotypes, merit further studies involving both morphological and molecular data.

Hybridization in Populations Studied—Natural hybridization between individuals of wild populations from *Tragopogon* has been reported in many studies on the basis of both morphology and molecular data (e.g. cf. Ownbey 1950; Díaz de la Guardia and Blanca 2004; Mavrodiev et al. 2008b). The combination of morphological and molecular data is a powerful tool for detecting instances of hybridization, especially recent hybridization. In the present study, we detected several putative hybrid populations involving *T. dubius*, *T. lainzii*, and *T. porrifolius* on the basis of the morphological and molecular features. Moreover, the inclusion in the molecular analyses of a chloroplast region has allowed us to suggest which species are the maternal parents. Ownbey (1950), in his study of natural allopolyploid formation involving introduced *Tragopogon* species in North America, stated that natural hybrids can be expected wherever any of these species grow together. For each of the hybrids we detected, the two parental species were growing together (RIO: *T. dubius* and *T. lainzii*; CH and CAZ: *T. dubius* and *T. porrifolius*).

In all three hybrid populations, the individuals showed a combination of the morphological features typical of the parental species, and few characters showed intermediate forms. Thus, in the population where *T. dubius* and *T. lainzii* occur together, the hybrids detected always show the floral and leaf features of *T. lainzii*, and therefore they look like *T. lainzii*. However, achene characters were more variable. In this population, some individuals had the achene type of *T. dubius* and others the achene type of *T. lainzii*, and intermediate forms between them were detected. Our results obtained from the chloroplast *rpl16* region suggest that in this population *T. lainzii* acts as the maternal parent.

With regard to the hybridization detected in those populations where *T. dubius* and *T. porrifolius* grow together, the results suggest *T. porrifolius* as the maternal parent (consistent with the maternal parentage of the allotetraploid *T. mirus*, which is derived from *T. dubius* and *T. porrifolius*; Soltis and Soltis 1989). Contrary to Ownbey's observations (1950), nonbicolored ligules were detected in the hybrids, but they look like either parental species (yellow ligules in the CH population, and purple ligules in the CAZ population). Unlike ligule color, the achene characters are good markers to distinguish hybrids between *T. dubius* and *T. porrifolius*. *Tragopogon porrifolius* has a characteristic subcylindric beak-apex shape (club-shaped in *T. dubius*; Blanca and Díaz de la Guardia 1997), which is a good hybridization marker when it appears in *T. dubius*-like hybrids. The club-shaped beak-apex is also a good hybridization marker when it appears in *T. porrifolius*-like hybrids.

The diploid hybrids studied by Ownbey (1950) were highly sterile, as their heads did not continue to develop normally after flowering, and almost all ovaries aborted at the flowering stage or shortly thereafter. Based on this evidence, together with the morphological uniformity of the hybrids, Ownbey inferred that these hybrids were F_1 individuals. Although we did not carry out an exhaustive analysis of hybrid sterility, all individuals sampled from the hybrid populations were fertile; they showed normal heads, and their seeds germinated normally (pers. obs.). These observations, together with the floral features (flower like *T. lainzii* in *T. dubius* × *T. lainzii* plants, and nonbicolored flowers in *T. dubius* × *T. porrifolius* individuals) and the range of variation in the achene characters, would suggest that the hybrids of these populations are not F_1 plants, but may represent later-generation backcrosses to one parent.

Finally, hybridization seems to be a frequent phenomenon in *T. dubius* populations where it grows together with other species (e.g. cf. Ownbey 1950). Hybridization should be considered as a possible source of variation when studies of the genus *Tragopogon* are conducted, especially in those studies including molecular markers, in which the use of a "hybrid" plant that is not recognized as such can yield mistaken conclusions. Thus, the combination of morphology and molecular markers is a useful approach for detecting hybridization.

Taxonomic Treatment

Tragopogon lainzii V. N. Suárez-Santiago, P. S. Soltis, D. E. Soltis, C. Díaz de la Guardia & G. Blanca sp. nov.—TYPE: SPAIN. Granada: ctra. Orce-María, 950 m, 13 May 2006, *V. N. Suárez-Santiago and I. López-Flores 52778* (holotype: GDA). See Appendix 1 for additional specimens.

Differt a plus minusve simili *T. dubius* Scop. caulibus rubellis, foliis margine undulatis, bracteis involucralibus 13 atque post anthesin accrescentibus [ita ut 44(54.8 ± 0.3)66 mm longae fiant], per anthesin autem aequilongis aut brevioribus quam ligulis externis [hae quidem 30(37.3 ± 0.2)48 mm longae sunt] et achaeniis 115(186.3 ± 0.02)263 in capitulo unoquoque [rostrum achaenii uniuscuiusque 15.5(21.5 ± 0.2)27.5 mm longum, corpus autem 7.5(10.0 ± 0.1)11.5 item longum].

Biennial plants. Stems 30–80(–100) cm, ramose in the basal zone, glabrous, woolly-floccose pubescent in the leaf axils, reddish. Leaves linear, broadening at the base to form a sheath, margin entire and undulate; the basal leaves numerous, rosulate; the cauline leaves (10–)15–30(–35) × 1.5–2.2 cm, decreasing in size towards the apex, alternate, semiamplexicaul, largely subulate. Capitula homogamous, terminal, solitary; peduncles cylindrical, markedly swollen at the apex, 7–13 mm wide at anthesis, 12–20 mm in fruit; involucre with 13 bracts in one row; involucral bracts 27–45 × 4–9 mm at anthesis, 44–66 × 5–11 mm in fruit, lanceolate, subkeeled, glabrous, greenish. Ligules 30–48 mm long, as long as or longer than involucral bracts, pale-yellow, with dark veins on the back and teeth greenish-brown; anthers dark-brown and style greenish-brown. Achenes 25–38.5 mm long; body 7.5–11.5 mm, sligthly curved, scabrous, brown, gradually tapering towards the beak, beak 15.5–27.5 mm long, obpyramidal at the tip. Pappus 20–30 mm, with plumose hairs. $2n = 12$. (IV)V-VI(VII). Figure 3.

Etymology—The epithet honors our friend and colleague, the botanist P. Manuel Laínz, S. J.

Habitat—Grassy areas of nitrified lands, usually in road taluses and ditches, on carbonate-loamy substrate, 500–1,500 m SE of Iberian Peninsula.

Key to Yellow-Flowered Species of *Tragopogon* in the Iberian Peninsula

1. Involucral bracts 5(–7); achenes 17–25 mm long . . . 2
  2. Cauline leaves subulate, 0.3–0.5 cm wide; ligules 4/5 length of involucral bracts or almost the same; achenes 17–22 mm long . . . *T. pratensis*
  2. Cauline leaves linear-lanceolate, 0.6–0.8 cm wide; ligules 2/3 length of involucral bracts; achenes 20–25 mm long . . . *T. pseudocastellanus*
1. Involucral bracts (7–)8–13(–16); achenes 23–39 mm long . . . 3
    3. Peduncles contracted below the capitulum during fruiting; involucral bracts with reddish or blackish margin; florets yellow, with reddish-orange dorsal veins . . . *T. lamottei*
    3. Peduncles gradually swollen towards the capitulum, involucral bracts greenish; florets yellow . . . 4
      4. Leaf margin not undulate; ligules 2/3–1/2 length of involucral bracts . . . *T. dubius*
      4. Leaf margin undulate; ligules as long as or longer than involucral bracts . . . *T. lainzii*

Acknowledgments. The authors would like to thank Padre M. Laínz for assistance with the text in Latin. We are also grateful to the staff of the herbarium of the University of Granada, to the staff of the Marion Ownbey Herbarium, Washington State University, to Dr. K. Pistrick of the Leibniz-Institut für Pflanzengenetik und Kulturpflanzenforschung in Gatersleben, and to Dr. B. Gemeinholzer of the Botanischer Garten und Botanisches Museum Berlin-Dahlem, Freie Universität Berlin. We thank Dr. F. Alba-Sánchez and Dr. D. Nieto-Lugilde for assistance with Fig. 1. Dr. Suárez-Santiago was funded by a postdoctoral grant from the Spanish Ministry of Education and Science. This work was supported in part by NSF grants MCB-0346437 and DEB-06144421. We also thank two anonymous reviewers and Dr. Andrew Hipp for their comments.

Literature Cited

Akaike, H. 1973. Information theory and an extension of the maximum likelihood principle. Pp. 267–281 in *Second international symposium on information theory*, eds. B. N. Petran and F. Csaki. Budapest: Akademiai Kiado.

Baldwin, B. G. and S. Markos. 1998. Phylogenetic utility of the external transcribed spacers (ETS) of 18S–26S rDNA: congruence of ETS and ITS trees of *Calycadenia* (Compositae). *Molecular Phylogenetics and Evolution* 10: 449–463.

Blanca, G. and C. Díaz de la Guardia. 1996. Sinopsis del Género *Tragopogon* L. (Asteraceae) en la Península Ibérica. *Anales del Jardin Botanico de Madrid* 54: 358–363.

Blanca, G. and C. Díaz de la Guardia. 1997. Fruit morphology in *Tragopogon* L. (Compositae: Lactuceae) from the Iberian Peninsula. *Botanical Journal of the Linnean Society* 135: 319–329.

Bolòs, O. and J. Vigo. 1989. Notes sobre taxonomia i nomenclatura de plantes, IV. *Folia Botanica Miscellanea* 6: 85–86.

Chaubard, L. A. 1837. *Tragopogon* L. Pp. 395–397 in *Flore du bassin sous-pyrénéen*, ed. J. B. Noulet. Toulouse.

Darlington, C. D. and L. F. La Cour. 1969. *The handling of chromosomes*. London: Allen and Unwin.

Díaz de la Guardia, C and G. Blanca. 1990. *Tragopogon castellanus* Levier = *T. crocifolius* subsp. *badalii* Willk. *Anales del Jardin Botanico de Madrid* 47: 253–256.

Díaz de la Guardia, C and G. Blanca. 2004. A new Spanish species of *Tragopogon* (Asteraceae: Lactuceae). *Botanical Journal of the Linnean Society* 146: 505–511.

Doyle, J. J. and J. L. Doyle. 1987. A rapid DNA isolation procedure for small quantities of fresh leaf tissue. *Phytochemical Bulletin* 19: 11–15.

Dvořák, F., P. Trnka, and B. Dadáková. 1978. Cytotaxonomic study of *Tragopogon* L. in Czechoslovakia. *Folia Geobotanica et Phytotaxonomica* 13: 305–330.

Felsenstein, J. 1985. Confidence limits on phylogenies: an approach using the bootstrap. *Evolution* 39: 783–791.

Font Quer, P. 1979. *Diccionario de Botánica*. Barcelona: Labor.

Innis, M. A., D. H. Gelfand, J. J. Sninsky, and T. J. White. 1990. *PCR protocols: a guide to methods and applications*. New York: Academic Press.

Jacquin, N. J. 1773. *Florae Austriacae* vol. 1. Vienna: Viennae Austriae, Typis Leopoldi Joannis Kaliwoda, Aulae imperialis typographi.

Jordan, W. C., M. W. Courtney, and J. E. Neigel. 1996. Low levels of intraspecific genetic variation at a rapidly evolving chloroplast DNA locus in North American duckweeds (Lemnaceae). *American Journal of Botany* 83: 430–439.

Kluge, A. G. and J. S. Farris. 1969. Quantitative phyletics and the evolution of anurans. *Systematic Zoology* 40: 315–328.

Krahulec, F., Z. Kaplan, and J. Novák. 2005. *Tragopogon porrifolius* × *T. pratensis*: the present state of an old hybrid population in Central Bohemia, the Czech Republic. *Preslia* 77: 297–306.

Lee, J., B. G. Baldwin, and L. D. Gottlieb. 2002. Phylogeny of *Stephanomeria* and related genera (Compositae–Lactuceae) based on analysis of 18S–26S nuclear rDNA ITS and ETS sequences. *American Journal of Botany* 89: 160–168.

Levan, A., K. Fredga, and A. A. Sandberg. 1964. Nomenclature for centromeric position on chromosomes. *Hereditas* 52: 201–220.

Lindemann, E. E. 1881. *Flora Chersonensis* vol. 1. Stockholm: Odessae.

Lutzoni, F., P. Wagner, V. Reeb, and S. Zoller. 2000. Integrating ambiguously aligned regions of DNA sequences in phylogenetic analyses without violating positional homology. *Systematic Biology* 49: 628–651.

Mavrodiev, E. V., I. Nawchoo, P. S. Soltis, and D. E. Soltis. 2008a. Molecular data reveal that the tetraploid *Tragopogon kashmirianus* (Asteraceae: Lactuceae) is distinct from the North American *T. mirus*. *Botanical Journal of the Linnean Society* 158: 391–398.

Mavrodiev, E. V., P. S. Soltis, M. A. Gitzendanner, R. M. Baldini, and D. E. Soltis. 2007. Polyphyly of *Tragopogon porrifolius* (Asteraceae), a Eurasian native with intercontinental disjuncts. *International Journal of Plant Sciences* 168: 889–904.

Mavrodiev, E. V., P. S. Soltis, and D. E. Soltis. 2008b. Putative parentage of six old world polyploids in *Tragopogon* L. (Asteraceae: Scorzonerinae) based on ITS, ETS, and plastid sequence data. *Taxon* 57: 1215–1232.

Mavrodiev, E. V., M. Tancig, A. M. Sherwood, M. A. Gitzendanner, J. Rocca, P. S. Soltis, and D. E. Soltis. 2005. Phylogeny of *Tragopogon* L. (Asteraceae) based on internal and external transcribed spacer sequence data. *International Journal of Plant Sciences* 166: 117–133.

Nylander, J. A. A. 2004. MrModeltest v. 2. Program distributed by the author. Evolutionary Biology Centre, Uppsala University.

Ownbey, M. 1950. Natural hybridization and amphiploidy in the genus *Tragopogon*. *American Journal of Botany* 37: 487–499.

Ownbey, M. and G. D. McCollum. 1953. Cytoplasmic inheritance and reciprocal amphiploidy in *Tragopogon*. *American Journal of Botany* 40: 788–796.

Richardson, I. B. K. 1976. *Tragopogon* L. Pp. 322–325 in *Flora Europaea* vol. 4, eds. T. G. Tutin, V. H. Heywood, N. A. Burges, D. M. Moore, D. H. Valentine, S. M. Walters, and D. A. Webb. Cambridge: Cambridge University Press.

Ronquist, F. and J. P. Huelsenbeck. 2003. MRBAYES 3: Bayesian phylogenetic inference under mixed models. *Bioinformatics* 19: 1572–1574.

Small, R. L., J. A. Ryburn, R. C. Cronn, T. Seelanan, and J. F. Wendel. 1998. The tortoise and the hare: choosing between noncoding plastome and nuclear *Adh* sequences for phylogenetic reconstruction in a recently diverged plant group. *American Journal of Botany* 85: 1301–1315.

Soltis, D. E. and P. S. Soltis. 1989. Allopolyploid speciation in *Tragopogon*: Insights from chloroplast DNA. *American Journal of Botany* 76: 1119–1124.

Soltis, D. E., P. S. Soltis, J. C. Pires, A. Kovarik, and J. Tate. 2004. Recent and recurrent polyploidy in *Tragopogon* (Asteraceae): genetic, genomic, and cytogenetic comparisons. *Biological Journal of the Linnean Society. Linnean Society of London* 82: 485–501.

Stearn, W. T. 1980. *Botanical Latin*. London: David and Charles.

Stebbins, G. L. 1971. *Chromosomal evolution in higher plants*. London: Edward Arnold.

Swofford, D. L. 1993. PAUP: phylogenetic analysis using parsimony, v. 3.1.1. Champaign: Illinois Natural History Survey.

Swofford, D. L. 2003. PAUP*. Phylogenetic analysis using parsimony (*and other methods), v. 4.0. Sunderland: Sinauer Associates.

Tamura, K., J. Dudley, M. Nei, and S. Kumar. 2007. MEGA4: Molecular Evolutionary Genetics Analysis (MEGA) software version 4.0. *Molecular Biology and Evolution* 24: 1596–1599.

Thornill, J. W., R. K. Matta, and W. H. Wood. 1965. Examining three dimensional microstructures with the scanning electron microscope. *Grana Palynologica* 6: 3–6.

Tzvelev, N. N. 1985. Genus *Tragopogon* L. (Asteraceae) in the European part of the USSR. Pp. 238–250 in *News in higher plant systematics* vol. 22, ed. T. Egorova. Leningrad: Nauka.

Vollmann, F. 1914. *Flora von Bayern*. Stuttgart.

Wilgenbusch, J. C., D. L. Warren, and D. L. Swofford. 2004. AWTY: A system for graphical exploration of MCMC convergence in Bayesian phylogenetic inference. http://ceb.csit.fsu.edu/awty.

Wen, J. and E. A. Zimmer. 1996. Phylogeny and biogeography of *Panax* L. (the ginseng genus, Araliaceae): inference from ITS sequences of the nuclear ribosomal DNA. *Molecular Phylogenetics and Evolution* 6: 167–177.

Appendix 1. Population data, voucher information and type of analysis performed for taxa used in this study. Information is listed as follows: species: country: population code; locality; voucher data; type of analysis (M: morphological analysis, C: cytogenetical analysis, I: molecular analysis); EMBL accession number (in parenthesis). All specimens are deposited at GDA herbarium (University of Granada).

Tragopogon angustifolius*:** Spain: **A-92**; Granada, Autovía A-92, en la salida 303 a Hernán Valle; *V. N. Suárez-Santiago and I. López-Flores*, *13/V/2006*, *52757* (GDA); I (ETS: FN675685, ITS: FN675712, *rpl16*: FN687182). **ORC**; Granada, ctra. a Orce desde la ctra. comarcal 330; *V. N. Suárez-Santiago and I. López-Flores*, *13/V/2006*, *52722* (GDA); I (ETS: FN675684, ITS: FN675711, *rpl16*: FN687181). *T. dubius:** Spain: **AD**; Burgos, Aranda de Duero, Salida Sur, junto gasolinera CEPSA; *V. N. Suárez-Santiago and I. López-Flores*, *28/V/2006*, *52768* (GDA); M, C, I (ETS: FN675675, ITS: FN675703, *rpl16*: FN687175). **ALAR**; Palencia, Alar del Rey, junto vía del tren; *V. N. Suárez-Santiago and C. Abellán-López, 6/VII/2006*, *52776* (GDA); C, I (ETS: FN675669, ITS: FN675697). **AT**; Guadalajara, Atienza, monte detrás del pueblo; *V. N. Suárez-Santiago and C. Abellán-López, 30/VI/2006*, *52767* (GDA); M, C, I (*rpl16*: FN687170). **CAZ**; Jaén, Ctra. Peal de Becerro-Cazorla (A-319), prop. Cazorla, antes del cruce con A-322, 750 m; *V. N. Suárez-Santiago et al. 4/VI/2008, 55948* (GDA); C, I (ETS: FN675668, ITS: FN675698, *rpl16*: FN687168).**CH**; Granada, Sierra Nevada, La Cortichuela, Jardín Botánico, 1,650 m; *G. Blanca et al. 27/VI/2006*, *52773* (GDA); M, C, I (ETS: FN675677, ITS: FN675705, *rpl16*: FN687177). **LEN**; Burgos, nacional 114 entre Sigüenza y Aranda de Duero, 1 km pasado Aldealengua, a 30 km de Aranda de Duero; *V. N. Suárez-Santiago and C. Abellán-López, 30/VI/2006*, *52770* (GDA); M, C, I (ETS: FN675671, ITS: FN675701, *rpl16*: FN687171). **IZN**; Granada, Ctra Iznalloz-Guadahortuna (A-323) Km 2, entre las Encebras y el Navazuelo, 1,000 m; *V. N. Suárez-Santiago et al., 4/VI/2008, 54994* (GDA); M, C, I (ETS: FN675670, ITS: FN675696, *rpl16*: FN687169). **OAS**; Jaén, Ctra. Jaén-Granada (A-44), estación de servicio el Oasis, junto gasolinera; *V. N. Suárez-Santiago and F. López-Soriano, 25/V/2008, 54996* (GDA); M, C, I (ETS: FN675672, ITS: FN675702, *rpl16*: FN687172). **SOM**; Madrid, Pto. Somosierra, Salida 79 hacia Horcajo de la Sierra, Ctra. entre Horcajo de la Sierra y Montejo de la Sierra (M-141), 1,300 m; *V. N. Suárez-Santiago and S. Schiaffino*, *21/VI/2008, 54997* (GDA); M, C, I (ETS: FN675673, ITS: FN675699, *rpl16*: FN687173). **SOR**; Soria, Nacional 122 entre el Burgo de Osma y Soria, km 206-205; *V. N. Suárez-Santiago and C. Abellán-López, 1/VII/2006, 52777* (GDA); C, I (ETS: FN675676, ITS: FN675704, *rpl16*: FN687176). **TOB**; Ctra. Ocaña-Albacete (N-301), Villatobas, 1km pasado el pueblo, 600 m; *V. N. Suárez-Santiago and S. Schiaffino*, *20/VI/2008, 54998* (GDA); M, C, I (ETS: FN675674, ITS: FN675700, *rpl16*: FN687174). ***T. lainzii*:** Spain: **CASTR**; Granada, Sierra de Castril, río Castril, 950 m; *V. N. Suárez-Santiago et al., 19/VI/2008, 54992* (GDA); M, C, I (ETS: FN675663, ITS: FN675691, *rpl16*: FN687159). **CAZ**; Jaén, Ctra. Peal de Becerro-Cazorla (A-319), prop. Cazorla, antes del cruce con A-322, 750 m; *V. N. Suárez-Santiago et al., 54993* (GDA); M, C, I (ETS: FN675666, ITS: FN675694, *rpl16*: FN687167). **FAD**; Granada, entre la Cañada de Cañepla y la Puebla de Don Fadrique; ctra. A-317 (prop. La Puebla); *V. N. Suárez-Santiago and I. López-Flores*, *13/V/2006*, *52775* (GDA); M, C, I (ETS: FN675658, ITS: FN675686, *rpl16*: FN687160). **JOD**; Jaén, Ctra. Jódar-Peal de Becerro (A-322), 450 m; *V. N. Suárez-Santiago et al., 4/VI/2008, 54986* (GDA); M, C, I (ETS: FN675662, ITS: FN675690, *rpl16*: FN687163). **ORC**; Granada, ctra. Orce-María, 950 m; *V. N. Suárez-Santiago and I. López-Flores, 13/V/2006, 52778* (GDA); M, C, I (ETS: FN675664, ITS: FN675692, *rpl16*: FN687161). **PUCAST**; Granada, Sierra de Castril, Ctra. Pozo Alcón-Castril (A-326), prop. embalse de la Bolera. 950 m; *V. N. Suárez-Santiago et al., 19/VI/2008, 54990* (GDA); M, C, I (*rpl16*: FN687164). **PZ**; Jaén, Sierra del Pozo, Loma de Cagasebo; *V. N. Suárez-Santiago and G. Blanca, 14/VI/2006, 52774* (GDA); C, I (ETS: FN675665, ITS: FN675693, *rpl16*: FN687162). **RIO**; Albacete, Srra de Alcaraz; Ctra. entre Salobre y Riópar (CM-412), prop. Riópar, junto cruce con Ctra. C-415 hacia ptos. Crucetas y Crucetillas, 1,100 m; *V. N. Suárez-Santiago et al., 4/VI/2008, 54989* (GDA); M, C, I (ETS: FN675667, ITS: FN675695, *rpl16*: FN687165). **SAL**; Albacete, Sierra de Alcaraz, ctra. entre Salobre y Riópar (CM-412), entre Las Parideras y Las Dehesas, 1,000 m; *V. N. Suárez-Santiago et al., 4/VI/2008, 55104* (GDA); M, C, I (ETS: FN675660, ITS: FN675688). **SAG**; Granada, Sierra de la Sagra, Cortijo Casa de la Virgen. 1,350 m; *V. N. Suárez-Santiago et al., 4/VI/2008, 55001* (GDA); M, C, I (ETS: FN675661, ITS: FN675689). **SR**; Albacete, Sierra de Alcaraz, ctra entre Siles y Riópar; *V. N. Suárez-Santiago, and G. Blanca, 15/VI/2006, 52772* (GDA); C, I (ETS: FN675659, ITS: FN675687, *rpl16*: FN687166). ***T. porrifolius*:** Spain: **CARO**; Jaén, La Carolina, ctra. al Centenillo; *V. N. Suárez-Santiago and I. López-Flores, 19/V/2006, 52796* (GDA); I (ETS: FN675678, ITS: FN675709, *rpl16*: FN687179). **CAZ**; Jaén, Ctra. Peal de Becerro-Cazorla (A-319), prop. Cazorla, antes del cruce con A-322, 750 m; *V. N. Suárez-Santiago and S. López-Vinyallonga, 4/VI/2009, 55103* (GDA); M, C, I (ETS: FN675683, *rpl16*: FN687180). **CH**; Granada, Sierra Nevada, La Cortichuela, Jardín Botánico, 1,650 m; *V. N. Suárez-Santiago et al., 12/VI/2008, 54961* (GDA); C, I (ETS: FN675679, ITS: FN675706, *rpl16*: FN687178). **IZN**; Granada, Ctra Iznalloz-Guadahortuna (A-323) Km 2, entre las Encebras y el Navazuelo, 1,000 m; *V. N. Suárez-Santiago et al., 4/VI/2008, 54962* (GDA); C, I (ETS: FN675680, ITS: FN675707). **OAS**; Jaén, ctra. Jaén-Granada (A-44), estación de servicio el Oasis, junto gasolinera; *V. N. Suárez-Santiago and F. López-Soriano, 25/V/2008, 54954* (GDA); C, I (ETS: FN675681, ITS: FN675710). **ORC**; Granada, carretera Cúllar-Orce, dirección Orce desde comarcal 330; *V. N. Suárez-Santiago et al., 14/V/2008, 54963* (GDA); C, I (ETS: FN675682, ITS: FN675708).